Sleep Slow Oscillation-Spindle Coupling Precedes Spindle-Ripple Coupling During Development

Julia Fechner[1,*], María P. Contreras[1,*,#], Candela Zorzo[1,2], Xia Shan[1], Jan Born[1,3,4,5,†] and Marion Inostroza[1,†]

[1] Institute of Medical Psychology and Behavioral Neurobiology, University of Tübingen, Tübingen, Germany

[2] Laboratory of Neuroscience, Department of Psychology, Instituto de Neurociencias del Principado de Asturias (INEUROPA), University of Oviedo, Plaza Feijoo, Oviedo, Spain.

[3] German Center for Diabetes Research (DZD), Institute for Diabetes Research & Metabolic Diseases of the Helmholtz Center Munich at the University Tübingen (IDM), Germany

[4] Werner Reichert Center for Integrative Neuroscience, University of Tübingen, Tübingen, Germany

[5] German Center for Mental Health (DZPG), partner site Tübingen, Germany

* shared first authorship

[#] Present address: Leibniz Institute of Neurobiology, Magdeburg, Germany

† shared senior authorship

Correspondence to: Marion Inostroza or Jan Born

Emails: marion.inostroza@uni-tuebingen.de, jan.born@uni-tuebingen.de

Study Objectives

Sleep supports systems memory consolidation through the precise temporal coordination of specific oscillatory events during slow-wave sleep (SWS), i.e., the neocortical slow oscillations (SOs), thalamic spindles, and hippocampal ripples. Beneficial effects of sleep on memory are also observed in infants, although the contributing regions, especially hippocampus and frontal cortex, are immature. Here, we examined in rats the development of these oscillatory events and their coupling during early life.

Methods

EEG and hippocampal local field potentials (LFPs) were recorded during sleep in male rats at postnatal days (PD)26 and 32, roughly corresponding to early (1-2 years) and late (9-10 years) human childhood, and in a group of adult rats (14-18 weeks, corresponding to ~22-29 years in humans).

Results

SO and spindle amplitudes generally increased from PD26 to PD32. In parallel, frontocortical EEG spindles increased in density and frequency, while changes in hippocampal ripples remained non-significant. The proportion of SOs co-occurring with spindles also increased from PD26 to PD32. Whereas parietal cortical spindles were phase-locked to the depolarizing SO-upstate already at PD26, over frontal cortex SO-spindle phase-locking emerged not until PD32. Co-occurrence of hippocampal ripples with spindles was higher during childhood than in adult rats, but significant phase-locking of ripples to the excitable spindle troughs was observed only in adult rats.

Conclusions

Results indicate a protracted development of synchronized thalamocortical processing specifically in frontocortical networks (i.e., frontal SO-spindle coupling). However, synchronization within thalamocortical networks generally precedes synchronization of thalamocortical with hippocampal processing as reflected by the delayed occurrence of spindle-ripple phase-coupling.

Keywords

Development, spindles, slow oscillation, ripple, hippocampus, cortex

Statement of Significance

Memory consolidation during sleep is mediated by a dialogue between hippocampal and neocortical networks, which is known to depend on the synchronized occurrence of hippocampal ripples and thalamocortical slow oscillations and spindles. When this temporal coupling between sleep oscillatory events emerges during early life, when the hippocampus and frontal cortex are still immature, is unknown. In a rat model we recorded neocortical EEGs and hippocampal local field potentials at times corresponding to early and late childhood, and in adult animals. We found that although already during childhood, slow oscillations, spindles, and ripples often co-occur, a precise phase-coupling especially of ripples to the spindle oscillations, occurs rather late during development. This suggests that the mechanisms of sleep-dependent memory formation during early life may differ from those during adulthood.

Introduction

Sleep is a dynamic process that plays a critical role in brain development [1,2] and long-term memory formation [3,4], and respective underlying plastic changes [5,6]. The consolidation of memory during sleep is likely achieved by an active systems consolidation process in which episodic memories anchored in hippocampal networks, are gradually transformed into more abstract semantic memories residing mainly in neocortical networks [3,7]. Growing evidence supports the idea that this transformation of memory into semantic representations in neocortex is essentially mediated by the precise phase-coupling of three cardinal rhythms of slow wave sleep (SWS), i.e., the <1.5 Hz neocortical slow oscillations (SOs), the 10-16 Hz thalamic spindles, and the ~180 Hz hippocampal ripples. The SO comprising a downstate of global network hyperpolarization and neuronal silence followed by a depolarizing upstate of distinctly increased excitability, tends to nest a spindle phase-locked into its upstate [8,9]. In turn, thalamic spindles spread not only to the neocortex but, via different possible routes (e.g., the nucleus reunions, entorhinal cortex), also to hippocampal networks [10-12], where they tend to nest in the excitable troughs of their oscillations hippocampal ripples that accompany the replay of memories in hippocampal cell ensembles. This cross-frequency triple coupling of SOs to spindles to ripples presumably gates the transfer of newly acquired hippocampal memory information to the neocortex, thereby consolidating representations into neocortical networks [13–16].

While neuronal mechanisms of systems memory consolidation and memory transformation during sleep have been mainly explored in the mature brain, there is growing evidence that sleep supports the formation of memory also in the developing brain [17–19], although major regions contributing to this transformation process, like the hippocampus and prefrontal cortex, are still rather immature [20–23]. Indeed, the immaturity of the contributing cortical and hippocampal structures might also implicate an immature and less effective communication between the structures, as it is implemented by the synchronized occurrence of SOs, spindles and ripples during sleep. In human children, the coupling of spindles with SO upstates increased with age [24], together with an increased sleep-dependent gain in memory formed overnight [25,26], and in children between 7 and 15 years, a

closer SO-spindle coupling was positively associated with overnight memory consolidation, also independently of the children's age [27]. However, these studies only included school-age and older children and, moreover, did not cover hippocampal ripples which cannot be detected in the surface EEG.

Against this backdrop, the present experiments addressed the question to what extent the coupling between SO, spindles, and hippocampal ripples that is assumed to mediate systems consolidation processes during sleep, is present already at even earlier developmental stages than those examined in those forgoing studies. Because we were particularly interested in the dynamics of hippocampal ripples which cannot be identified in surface EEG recordings in humans, we adopted a rat model allowing the simultaneous recording of SOs and spindles in the surface EEG in conjunction with ripples as well as spindles in hippocampal local field potential (LFP) recordings.

In the following, we report results from studies in rats which were recorded during SWS twice, i.e., at postnatal day (PD)26 and PD32, i.e., time points roughly corresponding to early (1-2 years) and late (9-10 years) childhood in humans (see [28,29] for the correspondence of ages in rats and humans). A group of adult animals (14-18 weeks, ~22-29 years) was examined as reference (see Methods, for detailed description of groups and recordings, and analyses). A main finding of our study is that robust spindle-ripple coupling occurs rather late during development and was not detectable in the recordings during childhood. We discuss the finding in the context of the active systems consolidation concept. Assuming that the coupling between these sleep oscillations is indispensable for effective memory formation during sleep, the concept appears to be particularly challenged by the absence of spindle-ripple coupling during early development.

Methods

Animals and experimental design

Experiments were performed in 8 young male Long Evans rats (53-95 gram, 25-32 days old), which were subjected to experimental recordings twice, i.e., on PD26 and on PD32. In addition, recordings were obtained in 5 adult rats (280-340 gram, 14-18 weeks old) which were recorded once around

PD120. All animals were provided from Janvier Labs (Le Genest St. Isle, France). Animals were kept on a 12-hour light/dark cycle with lights off at 19:00 h, with water and food available ad libitum. Young and adult animals were also used in previous experiments [30,31]. (Those experiments followed different research questions and their findings did not in any way conflict with the results of the present study). All experimental procedures were approved by the University of Tübingen and the local institutions in charge of animal welfare (Regierungspräsidium Tübingen).

Surgical implantations

Standard surgical procedures were followed as described in [32]. Animals were anesthetized with an intraperitoneal injection of fentanyl (0.005 mg/kg BW), midazolam (2.0 mg/kg), and medetomidin (0.15 mg/kg). They were placed into a stereotaxic frame and supplemented with isoflurane (0.5%) when necessary. The scalp was exposed and holes were drilled into the skull for implanting 3 EEG screw electrodes: one frontal (adult animals: AP: +2.6 mm, ML: −1.5 mm, juvenile: AP: +3.0 mm, ML: -1.5 mm, relative to Bregma), one parietal (adult: AP: −2.0 mm, ML: −2.5 mm, juvenile: AP: -3.0 mm, ML: 2.5 mm), and an occipital reference electrode (adult: AP: −10.0 mm, ML: 0.0 mm, juvenile: AP: ~-10.0 mm, ML: ~-0.1 mm). For the recording of LFPs from the dorsal hippocampus (dHC), one additional electrode was implanted (adult: platinum, right, AP: −3.1 mm, ML: +3.0 mm, DV: −3.6 mm, juvenile: stainless steel left, AP: −3.0 mm, ML: +2.5 mm, DV: -2.5 mm). In the adult rats a further wire electrode was implanted into the right medial prefrontal cortex (data not reported here). LFP recordings were also referenced to the occipital screw electrode. Electrode positions were confirmed by histological analysis (Suppl. Figure S1). For EMG recordings, a stainless steel wire electrode was implanted in the neck muscle. Electrodes were connected to a six-channel electrode pedestal (PlasticsOne, USA) and fixed with cold polymerizing dental resin and the wound was sutured. Rats had at least 3 days (young) and 5 days (adult), respectively, for recovery.

Electrophysiological recordings and procedures

Sleep in young rats was recorded in a recording box (dark gray PVC, 30 × 30 cm, height: 40 cm) for two 3-hour intervals (separated by 5-min wake intervals) on four consecutive days. During the preceding

wake intervals, the young rats were free to explore objects in an open field. For the present analyses, we used recordings on the first and fourth day corresponding to PD26 and PD32 of the animals. In a subgroup of animals undergoing surgery one day earlier (i.e., on PD20 instead of PD21), recordings were also performed one day earlier. For simplicity and because exploratory analyses did not reveal any different dynamics in these animals, we refer here in all cases to the same time schema with PD26 and PD32 denoting the day of experimental recordings. Adult rats were subjected to the same procedure except that the 3-hour sleep intervals were not interrupted by a 5-min wake interval. All animals were habituated to the recording box for at least two days, twelve hours per day. All recordings took place during the light phase (between 7:30 am and 3:30 pm) while the animal's behavior was continuously tracked using a video camera. EEG, LFP and EMG signals were continuously recorded and digitalized using a CED Power 1,401 converter and Spike2 software (Cambridge Electronic Design, UK). During the recordings, the electrodes were connected to the amplifier through a swiveling commutator (Model 15A54, Grass Technologies, USA). Signals (all sampled at 1 kHz) were amplified and filtered between 0.1-300 Hz (EEG) and 30- 300 Hz (EMG). LFP recordings were high-pass filtered at 0.1 Hz.

Histology

After the last recording session, rats were terminally anesthetized with fentanyl (0.01 mg/kg of body weight), midazolam (4.0 mg/kg) and medetomidin (0.3 mg/kg). The electrodes positions were marked by electrolytic lesion (10 µA, 30 s; Suppl. Figure S1). Rats were perfused with physiological saline (50-100 ml for young rats, 200–300 ml for adult rats) followed by 4% paraformaldehyde (PFA, 200– 300 ml). After decapitation, the brains were removed and post-fixed in 4% PFA for one day. Coronal sections of 60 µm were cut using a vibratome, stained with 0.5% toluidine blue and examined under a light microscope. Due to incorrect electrode positioning, LFP data from 3 young animals had to be excluded from analysis.

Sleep stage classification

Sleep stages were determined offline based on EEG and EMG recordings, using standard visual scoring procedures for consecutive 10-s epochs as previously described in [33,34]. Three sleep stages were

discriminated: slow-wave sleep (SWS), preREM sleep and REM sleep. Wakefulness was identified by mixed-frequency EEG and sustained EMG activity, SWS by the presence of high amplitude low activity (delta activity: <4.0 Hz) and reduced EMG tone, REM sleep by low-amplitude EEG activity with predominant theta activity (5.0–10.0 Hz), phasic muscle twitches and decrease of EMG tone. PreREM was identified by a decreased delta activity, progressive increase of theta activity and presence of sleep spindles. Recordings were scored by two experienced experimenters (interrater agreement >89.9%). Consensus was achieved afterwards for epochs with divergent scoring.

Detection of slow oscillations, spindles and ripples

Before events were detected, periods contaminated by artifacts (including saturated amplifier channels) were discarded. Oscillatory target events were identified in the EEG and LFP using standard procedures as described previously [12,31,32]: In brief, for identification of SOs, EEG and LFP signals were filtered between 0.3-4.5 Hz, and an SO event was selected in the EEG if the following criteria were fulfilled: (a) two consecutive negative-to-positive zero crossings of the signal occurred at an interval between 0.4 and 2.0 s, (b) of these events in an individual rat and channel, the 35% with the highest negative peak amplitude between both zero crossings were selected and (c) of these events the 45% with the highest negative-to positive peak-to-peak amplitude were selected. For spindle detection, EEG and LFP signals were filtered between 7.0-20.0 Hz [13]. EEG signals were used for characterizing spindles and SO-spindle co-occurrence and coupling assumed to occur within thalamo-cortical circuitry, LFP signals were used to analyze spindle-ripple co-occurrences and coupling in hippocampal networks. Then, the envelope, i.e., the instantaneous amplitude, of the Hilbert transform on the filtered signal, was extracted followed by an additional smoothing (moving average with 200-ms window size). A spindle was identified when the absolute value of the transformed signal exceeded 1.5 standard deviations (SD) of the mean signal in the respective channel during the animal's SWS epochs, for at least 0.4 s and not more than 2.0 s. Spindle onset was defined by the time when the signal exceeded the 1.5 SD threshold the first time. Spindle amplitude was calculated as the integral of the envelope of the Hilbert-transformed signal between spindle onset and end. For calculating Hilbert

transformations, the MATLAB (MATLAB version 9.13.0.2105380 (R2022b) Update 2, The MathWork Inc., Natick, Massachusetts) function Hilbert was used. The envelope was extracted using the MATLAB function abs, which returns the absolute value (modulus), i.e., the “instantaneous amplitude” of the transformed signal. For detection of ripples in the dHC LFP, as described in [32] and [15], the signal was filtered between 150-250 Hz. To ensure removal of any technical artifacts in the ripple band, three additional bandstop filters were applied in the ranges of 147-152 Hz, 198-202 Hz and 248-252 Hz. Similar to the spindle detection, the Hilbert transform was calculated and the signal was smoothed using a moving average (window size 200 ms). A ripple event was identified when the smoothed Hilbert transform value exceeded a threshold of 2.5 SDs from the mean smoothed Hilbert transform of the filtered signal during an animal's SWS epochs, for at least 25 ms (including at least three cycles) and for not more than 500 ms.

For each individual rat and recording session, we analyzed different parameters to assess SO, spindle and ripple events. These parameters were for SO events: the mean peak-to-peak amplitude and density (per min SWS); for spindle events: amplitude (defined by the area under the curve of the smoothed Hilbert transform of the filtered EEG/LFP signal), density (per min), mean oscillatory frequency and duration; and for ripples, amplitude (defined by the area under the curve of the smoothed Hilbert transform of the filtered LFP signal), density (per min), mean oscillatory frequency, and duration.

Co-occurrence and phase-locking of oscillatory events

For analyzing the temporal relationships between SOs, spindles and ripples, we determined the number of spindle events occurring during an SO event and the number of ripples occurring during a spindle event. Spindles were counted as co-occurring with SOs, if the maximum value of the spindle oscillation occurred between onset and offset of an SO (as defined by the respective zero-crossings of the signal). Ripples were counted as co-occurring with spindles, if the entire ripple event occurred during a spindle.

Supplementing co-occurrence of events, we calculated the "preferred cycle phase", as a measure of the precise phase-coupling of spindles with SO events, and of the coupling of ripples with the spindle oscillation. For determining SO-spindle phase-coupling the raw EEG signal was filtered between 0.6-1.8 Hz, to account for the asymmetric shape of SOs (like in [15]). Visual inspection of confirmed a nearly sinusoidal shape of the resulting signal as well as the correspondence of the phases of the smoothed signal with the original signal (Fig. 1A). Then, the Hilbert transform was calculated on the filtered waveform, and the instantaneous phase of the SO at the spindle maximum was extracted. Correspondingly, for determining the spindle-ripple coupling, the raw LFP signal was filtered between 7-20 Hz, then, the Hilbert transform of each spindle that co-occurred with a ripple was calculated, and the instantaneous phase of the spindle at the time of a ripple maximum was extracted. For calculating the average preferred phase, we used the CircStat toolbox [37].

We performed two control analyses with regarding the phase-coupling analyses: As the Hilbert transform applied to the single events can introduce edging effects that subsequently bias determination of phase angles, we performed a control analysis based on Hilbert transforms of the full band-passed signal. These analyses (not reported here in detail) showed that edging effects introduced by Hilbert transforms of the events remained marginal and did in no ways bias phase-angle estimations. Another factor that may lead to inaccurate phase estimations is the use of rather wide frequency bands for coupling analyses. Accordingly, as our phase-coupling analyses with regard to spindle events relied on a rather wide (7-20 Hz) frequency band for the spindle events, we performed control analyses after splitting the band into sub-bands, i.e. 7-10, 10-12, 12-14, 14-17 and 17-20 Hz (see also Contreras et al. 2023). Then, for each individual spindle event, the corresponding filtered frequency sub-band was chosen to extract the phases (using also the "hilbert" and "angle" functions of MATLAB). Results from these analyses were the same as those based on the original wider 7-20 Hz band (and are not reported here).

Statistical analysis

Statistical analyses were performed using custom-written MATLAB scripts (MATLAB version 9.13.0.2105380 (R2022b) Update 2, The MathWork Inc., Natick, Massachusetts). To assess differences in SO, spindle and ripple characteristics and their co-occurrences, we used analyses of variance (ANOVA) including a between-groups factor 'age' (early childhood, late childhood, adulthood) and, for EEG parameters, 'topography' (frontal, parietal) as a repeated-measures factor. ANOVA were preceded by Levene's test for equality of variances to ensure that the assumption of homoscedasticity was met. ANOVA were followed by pairwise repeated-measures (for comparisons between early and late childhood) or independent samples t-tests (for comparison with the adult group). Additional ANOVA included a factor 'interval', reflecting that for all animals, recordings were obtained for two separate 3-hour intervals. Because these analyses did not indicate any significant interval-main or interaction effects, only results from data collapsed across both recording intervals will be reported here. For phase-locking analyses, we used the Rayleigh test and, as an additional, more liberal test also covering bi- and multimodal distributions, the Omnibus test (as implemented in CircStat toolbox [37]) to determine the phase(s) in the slow oscillation and spindle oscillation that locked the spindles and ripples, respectively. Because the resultant vector lengths were too small in our reported cases (i.e., < 0.45) for applying Watson-Williams tests to test for differences in the mean phase angle of coupling (as reflected by the resultant vector), we used a nonparametric approach, i.e., the multi-sample test for equal median directions, which is the circular analogue to the multi-sample Kruskal-Wallis-Test, to test for differences in median directions.

Results

Effects of age on characteristics of SOs, spindles and ripples

The time spent asleep and in the different sleep stages during the 3-hour recording intervals was roughly comparable at all ages ($p > 0.07$, for all parameters), with all animals spending most of the time in SWS (177.01 ± 9.65 min, across ages, Suppl. Table S1). Characteristics of the target oscillatory events are summarized in Table 1 and Supplementary Figure 2.

SO amplitude was higher in the parietal than frontal EEG ($F(1, 36) = 14.05$, $p < 0.001$, for topography main effect), and increased from early childhood (PD26) to maximum values at late childhood (PD32), and then again decreased towards adulthood (Figure 1, $F(2, 36) = 8.28$, $p < 0.005$, for age main effect, see Figure 1B, for pairwise comparisons between ages and frontal and parietal EEG). SO density (per min SWS) was likewise higher over parietal than frontal cortex, with this effect being most prominent at early childhood (PD26, $F(1, 36) = 15.21$, $p < 0.001$, for topography main effect, Figure 1C). There was no general effect of age on SO density ($p > 0.09$).

Spindle amplitude (determined as the area under the curve of the smoothed EEG Hilbert transform) increased at both frontal and parietal EEG sites from PD26 to PD32 ($F(2, 36) = 5.3$, $p < 0.01$ for main effect of age, Figure 1E). A parallel increase in spindle density ($F(2, 36) = 5.26$, $p < 0.01$) appeared to be more consistent in frontal recordings where spindle density was generally higher than in parietal recordings ($F(1, 36) = 131.19$, $p < 0.001$, for topography main effect, Figure 1F). Spindle frequency was distinctly higher at parietal than frontal recording sites in early childhood at PD26 (Figure 1G). At frontal sites, spindle frequency increased across childhood (PD32) and adulthood such that in adult rats, spindle frequency was comparable between sites ($F(2, 36) = 11.82$, $p < 0.001$, for age x topography interaction).

Hippocampal ripples did not significantly change in density, frequency or duration from PD26 to PD32 (for all relevant pairwise comparisons $p > 0.08$, Table 1). Ripple amplitude was reduced in the young rats (PD26 and PD32) in comparison with the adult rats ($F(2,12) = 10.08$, $p < 0.01$, for main effect of age, Figure 1I).

Temporal associations between SOs and spindles

We calculated the number of spindles co-occurring with SOs as well as the percentage of SO-spindle events with reference to the total number of identified SOs (set to 100 %). SO-spindle events occurred more often in the frontal than parietal EEG ($F(1,36) = 9.53$ and 27.84, $p < 0.01$, for absolute numbers and percentages of SO-spindle events, respectively). Both absolute numbers and percentages of SO-spindle events increased from early (PD26) to late childhood (PD32) and further increased towards

adulthood (F(2,36) = 42.6 and 27.50, P = 0.001, for respective main effects of age, see Figure 2A for pairwise comparisons). Particularly for the percentage of SO-spindle events, the age-associated increase was more pronounced over the frontal than parietal cortex (F(2, 36) = 4.04, $p < 0.05$, for age x topography interaction). An increase with age was likewise apparent when SO-spindle events were expressed as percentages of identified spindles (F(2,36) = 42.6 and 27.4 and 20.36, $p = 0.001$, for age main effects in frontal and parietal EEG, respectively). The age-dependent increase in SO-spindle events being likewise apparent for absolute numbers and percentages of SO-spindle events, indicates that this increase in the co-occurrence of SOs and spindles is entirely independent of changes in the density of the oscillations per se. It rather suggests that a more efficient way of temporally pairing SOs and spindles emerges with age.

In order to more precisely assess the time point when spindles occur during an SO, we determined the phase of the SO cycle to which spindles are time-locked to. (For these analyses the timing of a spindle was marked by the maximum trough of the spindle. However, basically the same results were obtained when spindle onset was used to mark the timing, see Supplementary Table 2.) Figure 2B depicts normalized angular histograms of spindle events relative to the SO-cycle phase, with the length and phase angle of the mean circular vector indicating the coupling strength, i.e., how consistently the spindles coupled to a certain SO phase across all SO events of all individual animals. Mean circular vectors indicated a significant phase-coupling of spindles to the upstate of identified SOs over parietal regions at all ages, i.e., on average at 21° on PD26, at 22° on PD32 and at 351° in the adult rats ($p < 0.001$, for Rayleigh test in each age group). Differences in the vector phase angle between age groups did not reach significance ($p = 0.062$, for the circular analogue of the Kruskal-Wallis test). Spindles in the frontal EEG were also phase-coupled to the SO upstate at late childhood (PD32, mean = 5°, $p < 0.001$, for Rayleigh test) and adult rats (mean = 12°, $p < 0.001$ for Rayleigh test) but not at early childhood (PD26; $p = 0.3824$ for Rayleigh test, 0.4982 for Omnibus test for bi- and multimodal distributions), indicating that at frontal sites the development of cross-frequency coupling between

cortical SO and thalamic spindles is protracted. The difference in the vector phase angle between PD32 and adult rats was not significant (p = 0.1974, circular analogue of the Kruskal-Wallis test).

Temporal associations between spindles and hippocampal ripples

We focused our analysis of spindle-ripple events on spindles that like ripples were identified in the hippocampal LFP signal. Reaching hippocampal networks, these LFP spindles were expected to most strongly couple hippocampal ripples. The number of ripples co-occurring during a spindle did not change from early (PD26) to late childhood (PD32) but, strongly decreased at adulthood (Figure 3A). This pattern was observed regardless of whether absolute counts of spindle-ripple events ($F(2,12) = 5.13$, $p < 0.05$, for effect of age), percentages with reference to the total number of spindles ($F(2,12) = 5.52$, $P < 0.05$) or percentages with reference to the total number of detected ripples were analyzed ($F(2,12) = 5.92$, $p < 0.05$). The decrease in spindle-ripple events in adulthood is, thus, independent of any age-associate dynamics in the occurrence of spindles or ripples itself. It stands in remarkable contrast with the co-occurrence of SO-spindle events exhibiting a distinct increase in adulthood (see Figure 2A). A significant decrease from childhood (PD26, PD32) to adulthood was likewise revealed in analyses of only those spindle-ripples events that occurred during a SO, i.e., on the triple occurrence of SO, spindles and ripples, with SOs identified either in frontal or parietal EEG recordings ($F(2,24) = 5.53$, $p < 0.05$, for age main effect in a 3 (age) x 2 (topography) ANOVA), although the overall number of such triple events in the 3 age conditions was relatively small.

We computed normalized (to the total number of ripples occurring during a spindle) phase histograms to quantify to what extent the occurrence of ripples during a spindle was coupled to a specific phase of the spindle oscillation (Figure 3B). The time of ripple occurrence in these analyses was indicated by the maximum peak of the ripple. In adult rats, ripples showed significant phase-coupling to the spindle oscillation with a mean angle of 329° ($p < 0.001$, Rayleigh test), corresponding to the down-to-upstate transition of the spindle oscillation. In contrast, during childhood ripples did not exhibit any significant phase-coupling with the spindle oscillation on PD26 (p = 0.97) or PD32 (p = 0.96). There was also no significant spindle-ripple phase coupling in any of the young rats in single

subject analyses of the individual rats on PD26 and PD32 (all $p > 0.1$, Rayleigh test), and the same picture was obtained when the cross-frequency coupling analyses were based on spindles detected in the parietal EEG signal, rather than in the hippocampal LFP signal. For spindles detected in the frontal EEG signal, no significant spindle-ripple coupling occurred at any age.

Discussion

We examined sleep slow oscillations (SOs), spindles and ripples and their temporal coupling during early development in rats on PD26 and PD32, roughly corresponding to early (1-2 years) and late (9-10 years) childhood in humans. We found a distinct developmental course for SOs and spindles, both reaching maximum amplitude at late childhood, and for spindles showing an increase in oscillatory frequency mainly in frontal cortex regions during childhood measures, which extends into adulthood. Features of hippocampal ripples remained remarkably stable across early and late childhood measurements but, were increased in amplitude at adulthood. Importantly, we observed distinct changes in the co-occurrence and coupling between these oscillatory events which emerged independently of the developmental changes observed for each single of these events. Numbers of SO-spindle events increased across childhood measurements and further towards adulthood. Spindles were consistently phase-coupled to the SO upstate at all ages, except during early childhood where no phase-coupling was revealed in recordings from frontal cortex. Diverging from the developmental dynamics of SO-spindle events, number of spindle-ripple events did not change across childhood measurements but distinctly decreased at adulthood. Despite of this decline in adulthood, cross-frequency coupling analysis revealed a robustly enhanced phase-coupling of ripples to the spindle oscillation only in the adult rats, but not at any of the childhood measurements. Collectively, the findings suggest that efficiently synchronized information processing during development is achieved distinctly earlier within thalamocortical networks than between hippocampal and thalamocortical networks.

Developmental changes in the central features of SOs and spindles observed in our rats, mimic the changes seen similarly during human early development. For the SOs, we found an increase in amplitude during childhood such that peak amplitudes were reached at late childhood (PD32) going into a decreased amplitude at adulthood. Very similar developmental courses with maximal SO amplitude during late childhood, were observed not only in other rodent studies [38], but also for SOs and related slow wave activity in human developmental studies [39]. SO amplitudes being higher in our rats in parietal than frontocortical EEG recordings, likely reflect the relatively smaller size of the frontal cortex in rats compared to humans who typically show higher SO amplitudes over frontal cortex [40]. SO density did not substantially change in our rats during childhood measurements. The changes in SOs, in particular the peak in SO amplitude around late childhood, has been linked to changes in synaptic connectivity in underlying cortical networks. Given that SO amplitude is positively correlated with synaptic density [41,42], maximum amplitudes reached during late childhood might reflect that developmental synaptogenesis reaches a maximum at the same time [43,44].

As to the thalamocortical spindles, we found a prominent increase in the oscillating frequency over childhood and adulthood, specifically for spindles recorded over the frontal cortex, which during childhood were also generally slower than those recorded from parietal cortex. This pattern also agrees with findings in humans showing an increase in spindle frequency in (early) childhood [45,46] as well as from childhood to adolescence [47,48]. Our pattern in rats appears to be also consistent with human findings indicating that frontal spindles undergo a sudden increase in the oscillating frequency during puberty [49-51], which then levels out in adulthood [46]. Also the increase in amplitude of frontal spindles across our childhood measurements with a subsequent decrease towards adulthood resembles the developmental pattern in humans where frontal spindle amplitude decreased only with or after puberty had started [49,50]. Finally, very similar to the human development of [45,47,50], spindle density in our rats increased across childhood (from PD26 to PD32) with this increase being more distinct over the frontal than parietal cortex. Divergences in spindle development between the rats of the present study and findings in humans appeared to pertain mainly to recordings over parietal

cortex. Thus, unlike humans who display a developmental increase in the oscillating frequency also for centroparietal spindles [52], in our rats frequency of parietal spindles did not change across ages. Also, contrasting with the distinct increase in amplitude of parietal spindles across childhood in rats, changes in parietal spindle amplitude across human childhood appear to be marginal [52]. The reasons for these discrepancies are not clear but, might be related to the fact that humans have more white matter than rodents and to the faster developmental increase in white matter in rodents than humans [53–58]. Whatever the case, overall the pattern of changes in rats shows clear similarities with that during human childhood for spindle development over frontal cortex and, importantly, hints at a differential developmental course for frontal and parietal cortical spindles that has been likewise observed in humans (e.g., [59]). An intriguing but open question in this context is to what extent these differences in developing spindles between frontal and parietal cortex correspond to the dissociation of so called "slow" and "fast" spindles observed in adult humans and rats that do not only show a similar topographical dissociation (frontal vs centroparietal) but differ also in function [60,61]. Overall, the multitude of similarities between spindle development during childhood in humans and rats underlines the validity of our rat model for exploring developmental changes in the sleep oscillatory events of interest.

Hippocampal ripples presently cannot be reliably measured by non-invasive EEG or MEG recordings which limits the direct exploration of their developmental course in humans. Studies in rodents that mainly focused on an even earlier postnatal age range than the present study, suggest that ripple amplitude, density and duration reach adult like levels already by PD24, i.e., before the childhood age range of interest in the present study [62,63]. The time course of ripple emergence during these early postnatal days appears to go in parallel with the switch in polarity (from membrane depolarization to hyperpolarization) of the effect of GABA-A receptor activation [64], as well as with the development of coordinated hippocampal replay of neuronal firing patterns that accompany these ripples [65] and which are thought of as a major mechanism driving memory consolidation during sleep [7]. Fitting the view that ripple development levels out already around PD24 we only found marginal

and altogether non-significant changes, e.g., a slight increase in ripple frequency and a decrease in ripple density across childhood measurements. This might surprise in light of evidence for continuing changes throughout childhood and adolescence in hippocampal inhibitory and excitatory synaptic transmission and ongoing neurogenesis [21,22]. We indeed observed a distinct increase in ripple amplitude at adulthood, suggesting that such changes continuously observed at the synaptic and circuit level [66,67] may accumulate over longer periods to eventually express at the network level during adolescence or early adulthood.

The temporal coupling of SOs, spindles and ripples is thought to be a mechanism that links replay of episodic memory information in hippocampal networks with memory processing in thalamocortical networks thereby promoting the integration of the hippocampally replayed information into neocortical long-term stores [3,7,68]. Against this backdrop, a central aim of our study was to explore the development across childhood of the temporal association between SOs and spindles and between spindles and ripples, reflecting the efficacy of memory processing *within* the thalamocortical system and *between* hippocampal and thalamocortical networks, respectively. Remarkably, we observed distinct developmental changes across childhood and into adulthood for the co-occurrence and phase-coupling of both spindles with SOs as well as of ripples with spindles. Frontocortical SO-spindle coupling increased from early to late childhood whereas significant spindle-ripple coupling was revealed only at adulthood. Importantly, the changes in SO-spindle as well as spindle-ripple co-occurrence were revealed regardless of whether absolute event numbers or percentages of the respective events (e.g., SO-spindle percentages relative to the total numbers of SOs or to the total numbers of spindles) were analyzed which indicates that the observed developmental changes in the temporal association between the events basically emerged independently of changes in the occurrence rate of each single oscillatory event.

The increase in SO-spindle events and in phase-coupling strength from early to late childhood in our rats agrees with evidence in humans indicating a region- and frequency-specific increase in sleep EEG coherence from 2 to 5 years of age [69]. In older school-children (9-16 years), SO-spindle coupling

strength increased with age in parallel with overnight memory gains [26,27]. In combination these and the present findings, thus, suggest a rather extended time course for the development of effective SO-spindle coupling which, on the one side, does not reach a plateau before adolescence and, on the other side, has already started during early childhood. In our rats, significant SO-spindle phase coupling was missing over frontal cortex at the earliest time point (PD26) concurring with evidence that the frontal cortex shows a protracted development in comparison with more posterior cortex [70]. The weaker coupling of spindles to SO upstates at this age might reflect a delayed myelinization [71] of, e.g., thalamo-frontocortical fibers, although other factors, such as the rather protracted development of the GABAergic system extending into late adolescence, may also contribute [72,73].

Unlike SO-spindle events, the number of spindle-ripples events remained at a stable level during childhood and was distinctly decreased at adulthood. This decline at adulthood was likewise apparent for the triple co-occurrence of SO-spindles with ripples. In parallel, significant phase-coupling of ripples to the spindle oscillation was absent at both early and late childhood measurements but, interestingly, it emerged - on a background of greatly diminished numbers of spindle-ripple events – in the adult rats. Thus, although during childhood more ripples co-occurred with spindles, only in adulthood this co-occurrence is synchronized such that ripples robustly coupled to a preferred phase of the spindle oscillation. It seems like in adulthood less event pairs are needed for efficient hippocampal-to-thalamocortical information transfer and, ultimately, for consolidating respective information into long-term memory. The temporal association of hippocampal ripples with spindles being rather stable during childhood but distinctly changing only at adulthood, moreover, suggests a rather delayed development of effective cross-regional communication between hippocampus and thalamocortical networks extending into early adulthood.

The cross-frequency coupling between oscillatory events has been proposed as an indicator most closely reflecting optimized information transmission between networks [74,75]. If so, the early presence of SO-spindle phase-coupling together with the persisting absence of significant spindle-ripple phase-coupling during early and late childhood measurements, suggests that the interregional

communication between hippocampus and thalamocortical networks functionally matures distinctly later in life than that within thalamocortical networks. However, given the limitations of our study, we have to caution against premature conclusions. Statistical power of our study was limited due to the rather small size of our sample of juvenile rats that, in addition, were kept in standard animal facilities, i.e., in conditions of impoverished stimulation. Previous work has shown that exposing infant rats to spatial experience specifically accelerates the sleep-associated emergence of spindle-ripple coupling during development [30]. Accordingly, the present study may overestimate the delay at which distinct spindle-ripple phase-coupling emerges during development. Another point to be considered here concerns our hippocampal LFP recordings using an occipital screw electrode as reference. This approach, favoring detection of larger ripple events considerably spreading across the network, is sensitive to confounding influences of age-related factors, such as differences in brain size and hippocampal size as well as in the thickness of the skull underlying the reference electrode. However, although such factors might have biased ripple amplitude measures, they are unlikely to substantially affect the coupling and phase-relationship between spindles and ripples, i.e., events measured in identical recording conditions. Moreover, to further exclude that differences in the intrahippocampal positioning of the electrodes confounded the observed age effects on hippocampal ripples, in supplementary analyses we compared effects just for the two electrodes best matching in location in the two age groups as well as for the two electrodes showing the greatest difference in location between the groups (Fig. S1). Both comparisons confirmed the pattern found for the entire groups, which rules out to a far extent confounding effects of differences in electrode locations between the age groups.

A further restriction of our study results from the lack of any behavioral measurement of memory. There is strong evidence for a causal contribution of hippocampal ripples [76,77] as well as of the coupling of spindles to the SO-upstate [14] to memory consolidation. By contrast, a causal contribution of the precise spindle-ripple phase-coupling to memory consolidation has been proposed mainly based on conceptual considerations. Presently, it cannot be excluded that such coupling

emerges as an epiphenomenon during development without behavioral relevance. Proving a causal role of spindle-ripple coupling requires that specifically the phase-coupling between the events is experimentally manipulated which is currently difficult to achieve but, might succeed in future studies based on the optogenetic induction of the oscillatory events (e.g., [14]).

In conclusion, in this study in developing rats we could not detect robust frontocortical SO-spindle coupling at PD26 and there was also no significant spindle-ripple coupling at both measures during childhood, i.e., PD26 and PD32. The absence of such coupling during early development can be considered a sign of immature communication between the participating structures, i.e., in the thalamocortical system in the case of SO-spindle coupling and between the thalamocortical system and hippocampus in the case of spindle-ripple coupling. Given ample evidence that memory consolidation substantially profits from sleep also in children and infants [7,17–20], the absence of robust spindle-ripple coupling during childhood measurements might be even taken to question the active systems consolidation concept which considers hippocampo-to-thalamocortical information transmission as a key mechanism supporting memory consolidation during sleep [3,7]. Conditions during early development might differ in that the mere temporal co-occurrence of spindles and ripples, without a precise phase-coupling, suffices for achieving effective consolidation.

Acknowledgements

The authors would like to thank I. Sauter for technical support, and Drs. Carlos Oyanedel and Ernesto Duran for help with conducting the experiments.

Disclosure Statement

This research was supported by grants from the Deutsche Forschungsgemeinschaft to M.I. (DFG In 279/2-1) and J.B. (DFG FOR 5434), and from the European Research Council (ERC AdG 883098 Sleep

Balance) to J.B. M.I. was supported by the Hertie Foundation (Hertie Network of Excellence in Clinical Neuroscience). Nonfinancial Disclosure: none.

Data availability

Data will be available upon reasonable request.

References

1. Graven SN, Browne J V. Sleep and Brain Development: The Critical Role of Sleep in Fetal and Early Neonatal Brain Development. *Newborn and Infant Nursing Reviews*. 2008;8(4):173-179. doi:10.1053/J.NAINR.2008.10.008
2. Marks GA, Shaffery JP, Oksenberg A, Speciale SG, Roffwarg HP. A functional role for REM sleep in brain maturation. *Behavioural Brain Research*. 1995;69(1-2):1-11. doi:10.1016/0166-4328(95)00018-O
3. Klinzing JG, Niethard N, Born J. Mechanisms of systems memory consolidation during sleep. *Nat Neurosci*. 2019;22(10):1598-1610. doi:10.1038/S41593-019-0467-3
4. Stickgold R. Sleep-dependent memory consolidation. *Nature 2005 437:7063*. 2005;437(7063):1272-1278. doi:10.1038/nature04286
5. Dang-Vu TT, Desseilles M, Peigneux P, Maquet P. A role for sleep in brain plasticity. *http://dx.doi.org/101080/13638490500138702*. 2009;9(2):98-118. doi:10.1080/13638490500138702
6. Tononi G, Cirelli C. Sleep and the Price of Plasticity: From Synaptic and Cellular Homeostasis to Memory Consolidation and Integration. *Neuron*. 2014;81(1):12. doi:10.1016/J.NEURON.2013.12.025
7. Brodt S, Inostroza M, Niethard N, Born J. Sleep—A brain-state serving systems memory consolidation. *Neuron*. 2023;111(7):1050-1075. doi:10.1016/J.NEURON.2023.03.005
8. Clemens Z, Mölle M, Eross L, Barsi P, Halász P, Born J. Temporal coupling of parahippocampal ripples, sleep spindles and slow oscillations in humans. *Brain*. 2007;130(11):2868-2878. doi:10.1093/BRAIN/AWM146
9. Mölle M, Marshall L, Gais S, Born J. Grouping of Spindle Activity during Slow Oscillations in Human Non-Rapid Eye Movement Sleep. *Journal of Neuroscience*. 2002;22(24):10941-10947. doi:10.1523/JNEUROSCI.22-24-10941.2002
10. Varela, C, and MA. Wilson. "mPFC spindle cycles organize sparse thalamic activation and recently active CA1 cells during non-REM sleep." *Elife* 9 (2020): e48881
11. Vertes, Robert P., et al. "Efferent projections of reuniens and rhomboid nuclei of the thalamus in the rat." *Journal of comparative neurology* 499.5 (2006): 768-796.
12. Sullivan, D., Mizuseki, K., Sorgi, A., & Buzsáki, G. Comparison of sleep spindles and theta oscillations in the hippocampus. *Journal of Neuroscience* (2014). 34(2), 662-674.
13. Fernandez LMJ, Lüthi A. Sleep Spindles: Mechanisms and Functions. *Physiol Rev*. 2020;100(2):805-868. doi:10.1152/PHYSREV.00042.2018
14. Latchoumane, C. F. V., Ngo, H. V. V., Born, J., & Shin, H. S. (2017). Thalamic spindles promote memory formation during sleep through triple phase-locking of cortical, thalamic, and hippocampal rhythms. *Neuron*, 95(2), 424-435.
15. Oyanedel CN, Durán E, Niethard N, Inostroza M, Born J. Temporal associations between sleep slow oscillations, spindles and ripples. *Eur J Neurosci*. 2020;52(12):4762-4778. doi:10.1111/EJN.14906
16. Staresina BP, Bergmann TO, Bonnefond M, et al. Hierarchical nesting of slow oscillations, spindles and ripples in the human hippocampus during sleep. *Nature Neuroscience 2015 18:11*. 2015;18(11):1679-1686. doi:10.1038/nn.4119
17. Friedrich M, Mölle M, Born J, Friederici AD. Memory for nonadjacent dependencies in the first year of life and its relation to sleep. *Nature Communications 2022 13:1*. 2022;13(1):1-10. doi:10.1038/s41467-022-35558-x
18. Friedrich M, Wilhelm I, Born J, Friederici AD. Generalization of word meanings during infant sleep. *Nature Communications 2015 6:1*. 2015;6(1):1-9. doi:10.1038/ncomms7004
19. Gómez RL, Bootzin RR, Nadel L. Naps Promote Abstraction in Language-Learning Infants. *https://doi.org/101111/j1467-9280200601764.x*. 2006;17(8):670-674. doi:10.1111/J.1467-9280.2006.01764.X

20. Casey BJ, Giedd JN, Thomas KM. Structural and functional brain development and its relation to cognitive development. *Biol Psychol*. 2000;54(1-3):241-257. doi:10.1016/S0301-0511(00)00058-2
21. Cossart R, Khazipov R. How development sculpts hippocampal circuits and function. *Physiol Rev*. 2022;102(1):343-378. doi:10.1152/PHYSREV.00044.2020/ASSET/IMAGES/LARGE/PHYSREV.00044.2020_F012.JPEG
22. Dumas TC. Late postnatal maturation of excitatory synaptic transmission permits adult-like expression of hippocampal-dependent behaviors. *Hippocampus*. 2005;15(5):562-578. doi:10.1002/HIPO.20077
23. Van Eden CG, Kros JM, Uylings HBM. Chapter 8 The development of the rat prefrontal cortex : Its size and development of connections with thalamus, spinal cord and other cortical areas. *Prog Brain Res*. 1991;85(C):169-183. doi:10.1016/S0079-6123(08)62680-1
24. Joechner, A. K., Hahn, M. A., Gruber, G., Hoedlmoser, K., & Werkle-Bergner, M. "Sleep spindle maturity promotes slow oscillation-spindle coupling across child and adolescent development." *Elife* 12 (2023): e83565.
25. Hahn MA, Heib D, Schabus M, Hoedlmoser K, Helfrich RF. Slow oscillation-spindle coupling predicts enhanced memory formation from childhood to adolescence. *Elife*. 2020;9:1-21. doi:10.7554/ELIFE.53730
26. Hahn M, Joechner A, Roell J, et al. Developmental changes of sleep spindles and their impact on sleep- dependent memory consolidation and general cognitive abilities: A longitudinal approach. *Dev Sci*. Published online 2019. doi:10.1111/desc.12706
27. Kurz EM, Zinke K, Born J. Sleep Electroencephalogram (EEG) Oscillations and Associated Memory Processing During Childhood and Early Adolescence. *Dev Psychol*. Published online 2022. doi:10.1037/DEV0001487
28. Sengupta, P. The laboratory rat: relating its age with human's. *International journal of preventive medicine*, 2013, 4(6), 624.
29. Quinn R. Comparing rat's to human's age: how old is my rat in people years*? Nutrition (Burbank, Los Angeles County, Calif)* 2005, 21:775–777.
30. Contreras MP, Fechner J, Born J, Inostroza M. Accelerating maturation of spatial memory systems by experience – evidence from sleep oscillation signatures of memory processing. *Journal of Neuroscience*. 2023: JN-RM-1967-22. doi:10.1523/JNEUROSCI.1967-22.2023
31. Durán E, Oyanedel CN, Niethard N, Inostroza M, Born J. Sleep stage dynamics in neocortex and hippocampus. *Sleep*. 2018;41(6):1-11. doi:10.1093/SLEEP/ZSY060
32. Mölle M, Yeshenko O, Marshall L, Sara SJ, Born J. Hippocampal sharp wave-ripples linked to slow oscillations in rat slow-wave sleep. *J Neurophysiol*. 2006;96(1):62-70. doi:10.1152/JN.00014.2006/ASSET/IMAGES/LARGE/Z9K0070675080006.JPEG
33. Neckelmann, Dag, et al. "The reliability and functional validity of visual and semiautomatic sleep/wake scoring in the Møll-Wistar rat." *Sleep* 17.2 (1994): 120-131.
34. Bjorvatn, Bjørn, Snorre Fagerland, and Reidun Ursin. "EEG power densities (0.5–20 Hz) in different sleep–wake stages in rats." *Physiology & Behavior* 63.3 (1998): 413-417.
35. Sawangjit A, Oyanedel CN, Niethard N, Salazar C, Born J, Inostroza M. The hippocampus is crucial for forming non-hippocampal long-term memory during sleep. *Nature*. 2018;564(7734):109-113. doi:10.1038/s41586-018-0716-8
36. Mölle M, Eschenko O, Gais S, Sara SJ, Born J. The influence of learning on sleep slow oscillations and associated spindles and ripples in humans and rats. *Eur J Neurosci*. 2009;29(5):1071-1081. doi:10.1111/J.1460-9568.2009.06654.X
37. Berens P. CircStat: A MATLAB Toolbox for Circular Statistics. *J Stat Softw*. 2009;31(10):1-21. doi:10.18637/JSS.V031.I10

38. Olini N, Huber R. Diurnal changes in electrocorticogram sleep slow-wave activity during development in rats. *J Sleep Res*. 2014;23(3):263-269. doi:10.1111/JSR.12124
39. Ringli M, Huber R. Developmental aspects of sleep slow waves: Linking sleep, brain maturation and behavior. *Prog Brain Res*. 2011;193:63-82. doi:10.1016/B978-0-444-53839-0.00005-3
40. Timofeev I, Grenier F, Bazhenov M, Sejnowski TJ, Steriade M. Origin of Slow Cortical Oscillations in Deafferented Cortical Slabs. *Cerebral Cortex*. 2000;10(12):1185-1199. doi:10.1093/CERCOR/10.12.1185
41. Feinberg I. Schizophrenia: Caused by a fault in programmed synaptic elimination during adolescence? *J Psychiatr Res*. 1982;17(4):319-334. doi:10.1016/0022-3956(82)90038-3
42. Peter R. H. Synaptic density in human frontal cortex — Developmental changes and effects of aging. *Brain Res*. 1979;163(2):195-205. doi:10.1016/0006-8993(79)90349-4
43. Turrigiano GG, Nelson SB. Hebb and homeostasis in neuronal plasticity. *Curr Opin Neurobiol*. 2000;10(3):358-364. doi:10.1016/S0959-4388(00)00091-X
44. Turrigiano GG, Nelson SB. Homeostatic plasticity in the developing nervous system. *Nature Reviews Neuroscience 2004 5:2*. 2004;5(2):97-107. doi:10.1038/nrn1327
45. Mcclain IJ, Lustenberger C, Achermann P, Lassonde JM, Kurth S, Lebourgeois MK. Developmental Changes in Sleep Spindle Characteristics and Sigma Power across Early Childhood. *Neural Plast*. 2016;2016. doi:10.1155/2016/3670951
46. Purcell SM, Manoach DS, Demanuele C, et al. Characterizing sleep spindles in 11,630 individuals from the National Sleep Research Resource. *Nature Communications 2017 8:1*. 2017;8(1):1-16. doi:10.1038/ncomms15930
47. Bocskai G, Pótári A, Gombos F, Kovács I. The adolescent pattern of sleep spindle development revealed by HD-EEG. *J Sleep Res*. 2022. doi:10.1111/JSR.13618
48. Zhang ZY, Campbell IG, Dhayagude P, Espino HC, Feinberg I. Longitudinal Analysis of Sleep Spindle Maturation from Childhood through Late Adolescence. *Journal of Neuroscience*. 2021; 41(19):4253-4261. doi:10.1523/JNEUROSCI.2370-20.2021
49. De Gennaro L, Ferrara M. Sleep spindles: An overview. *Sleep Med Rev*. 2003; 7(5):423-440. doi:10.1053/smrv.2002.0252
50. Nagata K, Shinomiya S, Takahashi K, Masumura T. Developmental characteristics of frontal spindle and centro-parietal spindle]. *No To Hattatsu = Brain and Development*. 1996; 28(5):409-417.
51. Scholle S, Zwacka G, Scholle HC. Sleep spindle evolution from infancy to adolescence. *Clin Neurophysiol*. 2007; 118(7):1525-1531. doi:10.1016/J.CLINPH.2007.03.007
52. Shinomiya S, Nagata K, Takahashi K, Masumura T. Development of Sleep Spindles in Young Children and Adolescents. *Clinical Electroencephalography. 1999*; 30(2).
53. Clawson BC, Durkin J, Aton SJ. Form and Function of Sleep Spindles across the Lifespan. *Neural Plast*. 2016. doi:10.1155/2016/6936381
54. Fogel S, Vien C, Karni A, Benali H, Carrier J, Doyon J. Sleep spindles: a physiological marker of age-related changes in gray matter in brain regions supporting motor skill memory consolidation. *Neurobiol Aging*. 2017; 49:154-164. doi:10.1016/J.NEUROBIOLAGING.2016.10.009
55. Gaudreault PO, Gosselin N, Lafortune M, et al. The association between white matter and sleep spindles differs in young and older individuals. *Sleep*. 2018; 41(9):1-13. doi:10.1093/SLEEP/ZSY113
56. Kurth S, Ringli M, Geiger A, LeBourgeois M, Jenni OG, Huber R. Mapping of Cortical Activity in the First Two Decades of Life: A High-Density Sleep Electroencephalogram Study. *The Journal of Neuroscience*. 2010; 30(40):13211. doi:10.1523/JNEUROSCI.2532-10.2010
57. Ventura-Antunes L, Mota B, Herculano-Houzel S. Different scaling of white matter volume, cortical connectivity, and gyrification across rodent and primate brains. *Front Neuroanat*. 2013; 7(MARCH). doi:10.3389/FNANA.2013.00003

58. Zhang K, Sejnowski TJ. A universal scaling law between gray matter and white matter of cerebral cortex. *Proc Natl Acad Sci USA*. 2000; 97(10):5621. doi:10.1073/PNAS.090504197
59. Gombos F, Bódizs R, Pótári A, et al. Topographical relocation of adolescent sleep spindles reveals a new maturational pattern in the human brain. *Scientific Reports.* 2022; *12:1*. 2022;12(1):1-10. doi:10.1038/s41598-022-11098-8
60. Ayoub A, Aumann D, Hörschelmann A, et al. Differential Effects on Fast and Slow Spindle Activity, and the Sleep Slow Oscillation in Humans with Carbamazepine and Flunarizine to Antagonize Voltage-Dependent Na+ and Ca2+ Channel Activity. *Sleep*. 2013; 36(6):905. doi:10.5665/SLEEP.2722
61. Mölle M, Born J. Slow oscillations orchestrating fast oscillations and memory consolidation. *Prog Brain Res*. 2011; 193:93-110. doi:10.1016/B978-0-444-53839-0.00007-7
62. Buhl DL, Buzsáki G. Developmental emergence of hippocampal fast-field "ripple" oscillations in the behaving rat pups. *Neuroscience*. 2005; 134(4):1423-1430. doi:10.1016/J.NEUROSCIENCE.2005.05.030
63. Farooq U, Dragoi G. Emergence of preconfigured and plastic time-compressed sequences in early postnatal development. *Science (1979)*. 2019; 363(6423):168-173.
64. Pignatelli M, Rockland KS. Organization and development of hippocampal circuits. *Neural Circuit and Cognitive Development*. 2020; 201-219. doi:10.1016/B978-0-12-814411-4.00009-3
65. Muessig L, Lasek M, Varsavsky I, Cacucci F, Wills TJ. Coordinated Emergence of Hippocampal Replay and Theta Sequences during Post-natal Development. *Current Biology*. 2019; 29(5):834. doi:10.1016/J.CUB.2019.01.005
66. Kempermann G, Jessberger S, Steiner B, Kronenberg G. Milestones of neuronal development in the adult hippocampus. *Trends Neurosci*. 2004 ; 27(8):447-452. doi:10.1016/J.TINS.2004.05.013
67. Li Y, Mu Y, Gage FH. Chapter 5 Development of Neural Circuits in the Adult Hippocampus. *Curr Top Dev Biol*. 2009; 87:149-174. doi:10.1016/S0070-2153(09)01205-8
68. Sawangjit A, Harkotte M, Oyanedel CN, Niethard N, Born J, Inostroza M. Two distinct ways to form long-term object recognition memory during sleep and wakefulness. *Proc Natl Acad Sci USA*. 2022; 119(34):e2203165119. doi:10.1073/PNAS.2203165119/SUPPL_FILE/PNAS.2203165119.SM01.MP4
69. Kurth S, Achermann P, Rusterholz T, Lebourgeois MK. Development of brain EEG connectivity across early childhood: Does sleep play a role? *Brain Sci*. 2013; 3(4):1445-1460. doi:10.3390/BRAINSCI3041445
70. Fuster JM. Frontal lobe and cognitive development. *J Neurocytol*. 2002. 31(3-5 SPEC. ISS.):373-385. doi:10.1023/A:1024190429920/METRICS
71. Mengler L, Khmelinskii A, Diedenhofen M, et al. Brain maturation of the adolescent rat cortex and striatum: Changes in volume and myelination. *Neuroimage*. 2014; 84:35-44. doi:10.1016/J.NEUROIMAGE.2013.08.034
72. Kilb W. Development of the GABAergic system from birth to adolescence. *Neuroscientist*. 2012; 18(6):613-630.
73. Kolk SM, Rakic P. Development of prefrontal cortex. *Neuropsychopharmacology. 2021; 47:1*. 2021;47(1):41-57. doi:10.1038/s41386-021-01137-9
74. Bergmann TO, Born J. Phase-Amplitude Coupling: A General Mechanism for Memory Processing and Synaptic Plasticity? *Neuron*. 2018; 97(1):10-13. doi:10.1016/J.NEURON.2017.12.023
75. Fries P. Rhythms For Cognition: Communication Through Coherence. *Neuron*. 2015; 88(1):220. doi:10.1016/J.NEURON.2015.09.034
76. Ego-Stengel V, Wilson MA. Disruption of ripple-associated hippocampal activity during rest impairs spatial learning in the rat. *Hippocampus*. 2010;20(1):1-10. doi:10.1002/HIPO.20707
77. Girardeau G, Benchenane K, Wiener SI, Buzsáki G, Zugaro MB. Selective suppression of hippocampal ripples impairs spatial memory. *Nature Neuroscience. 2009; 12:10*. 2009;12(10):1222-1223. doi:10.1038/nn.2384

Figures and Tables

Figure 1: **Characteristics of sleep oscillations at the different ages. (A)** Average SOs time-locked to downstate peak (0 ms) from parietal EEG EEG (solid lines). Dotted lines illustrate the average filtered (0.6 – 1.8 Hz) used for determining the phase of SO-spindle coupling. Light grey denotes PD26, mid-tone grey denotes PD32 and dark gray denotes PD120. **(B)** Mean±SEM SO peak-to-peak amplitude and **(C)** density (/min SWS). **(D)** Average spindle time-locked to maximum peak (0 ms) from parietal EEG. **(E)** Mean±SEM spindle amplitude, **(F)** density (/min SWS), and **(G)** oscillatory frequency. **(H)** Averaged ripple (time-locked to minimum peak, 0 ms) from hippocampal LFP recordings. **(I)** Mean ±SEM ripple amplitude. Frontal EEG - pink, parietal EEG - green, hippocampal LFP - orange. ** $P < 0.01$, * $P < 0.05$, for pairwise comparisons between ages, ## $P < 0.01$, # $P < 0.05$, for pairwise comparisons between frontal and parietal recordings.

Figure 2: Co-occurrences and phase-coupling of spindles with SOs at the different ages. (A) Mean (±SEM) absolute numbers (left) of spindles co-occurring with an SO (SO-spi events) and percentage (right) of SO-spindle events relative to total number of identified SOs, at frontal (pink) and parietal (green) EEG recording sites. ** $P < 0.01$, * $P < 0.05$, for pairwise comparisons between ages, ## $P < 0.01$, # $P < 0.05$, for pairwise comparisons between frontal and parietal EEG recordings. **(B)** Circular histograms showing, for the three ages and for frontal (upper row) and parietal EEG signals (lower row), the distribution of phase angles of the SO at which the spindles (maxima) occurred. The orientation and length of the mean circular vector (black) indicates the coupling strength, i.e., the consistency of the phase coupling of spindles to SOs across subjects at a certain age. Significance ($P < 0.0001$) of SO-spindle phase coupling is indicated by Rayleigh test for unimodal distributions. Phase coupling is significant at all ages and all recording sites, except for the recordings over frontal cortex on PD26 (early childhood). Right next to circular histograms, mean SO-spindle events are shown (SOs - blue, spindles - red, grey area indicates mean co-occurrence interval).

Figure 3: Co-occurrences and phase-coupling of ripples with spindles. (A) Mean ±SEM absolute numbers of spindle-ripple events (left) and percentage of spindle-ripple events relative to the total number of identified spindles (middle) and to the total number of identified ripples (right). Spindles and ripples were identified in the hippocampal LFP. ** $P < 0.01$, * $P < 0.05$, for pairwise comparisons between ages. **(B)** Circular histograms showing, for the three ages, the distribution of phase angles of the spindle oscillation at which ripples occurred. The length of the mean circular vector (black) indicates the coupling strength, i.e., the consistency of the phase-coupling of ripples to spindles across all spindles and rats at a certain age. The circle has a reference length of 0.01. Significance ($P < 0.0001$) of spindle-ripple phase coupling is indicated by Rayleigh test. Significant spindle-ripple phase-coupling is present only in adult rats. Right next to circular histograms, mean spindle-ripple events are shown (spindles - red, ripples - yellow, grey area indicates co-occurrence interval).

Table 1: Oscillatory characteristics over age

SOs	PD26	PD32	Adults
Amplitude (μV)			
Frontal EEG	351 ± 48	397 ± 77	285 ± 41
Parietal EEG	456 ± 123	537 ± 152	358 ± 39
Density (events/min)			
Frontal EEG	22.3 ± 0.9	22.7 ± 0.9	21.9 ± 1.1
Parietal EEG	24.1 ± 1.0	24.1 ± 1.6	22.9 ± 1.3
Frequency (Hz)			
Frontal EEG	1.62 ± 0.01	1.62 ± 0.01	1.65 ± 0.01
Parietal EEG	1.60 ± 0.01	1.62 ± 0.01	1.67 ± 0.01
Duration (s)			
Frontal EEG	0.68 ± 0.00	0.68 ± 0.01	0.66 ± 0.00
Parietal EEG	0.69 ± 0.01	0.68 ± 0.00	0.65 ± 0.00
Spindles			
Amplitude (mV^2/s)			
Frontal EEG	0.097 ± 0.009	0.113 ± 0.009	0.099 ± 0.017
Parietal EEG	0.088 ± 0.011	0.101 ± 0.014	0.108 ± 0.019
dHC LFP	0.314 ± 0.057	0.275 ± 0.076	0.467 ± 0.093
Density (events/min)			
Frontal EEG	1.96 ± 0.16	2.20 ± 0.10	2.29 ± 0.30
Parietal EEG	1.41 ± 0.23	1.48 ± 0.12	1.54 ± 0.20
dHC LFP	1.80 ± 0.10	1.52 ± 0.16	1.28 ± 0.20
Frequency (Hz)			
Frontal EEG	11.3 ± 0.3	11.5 ± 0.3	12.4 ± 0.3
Parietal EEG	12.6 ± 0.5	12.7 ± 0.4	12.3 ± 0.4
dHC LFP	11.2 ± 0.1	11.0 ± 0.2	11.5 ± 0.1
Duration (s)			
Frontal EEG	0.56 ± 0.01	0.58 ± 0.01	0.59 ± 0.01
Parietal EEG	0.53 ± 0.00	0.55 ± 0.01	0.54 ± 0.01
dHC LFP	0.54 ± 0.01	0.53 ± 0.01	0.52 ± 0.01
Ripples			
Amplitude (mV^2/s)			
dHC LFP	0.69 ± 0.23	0.57 ± 0.13	1.57 ± 0.61
Density (events/min)			
dHC LFP	9.50 ± 1.40	9.28 ± 2.02	5.26 ± 4.32
Frequency (Hz)			
dHC LFP	178.3 ± 5.6	180.7 ± 5.9	182.3 ± 4.0
Duration (s)			
dHC LFP	0.10 ± 0.01	0.12 ± 0.03	0.08 ± 0.01

Table 1: Mean (±SEM) amplitude, event density, oscillatory frequency and duration of SOs, spindles (recorded in the EEG over frontal and parietal cortex), and of hippocampal ripples (recorded in the LFP from dorsal hippocampus dHC) during SWS.

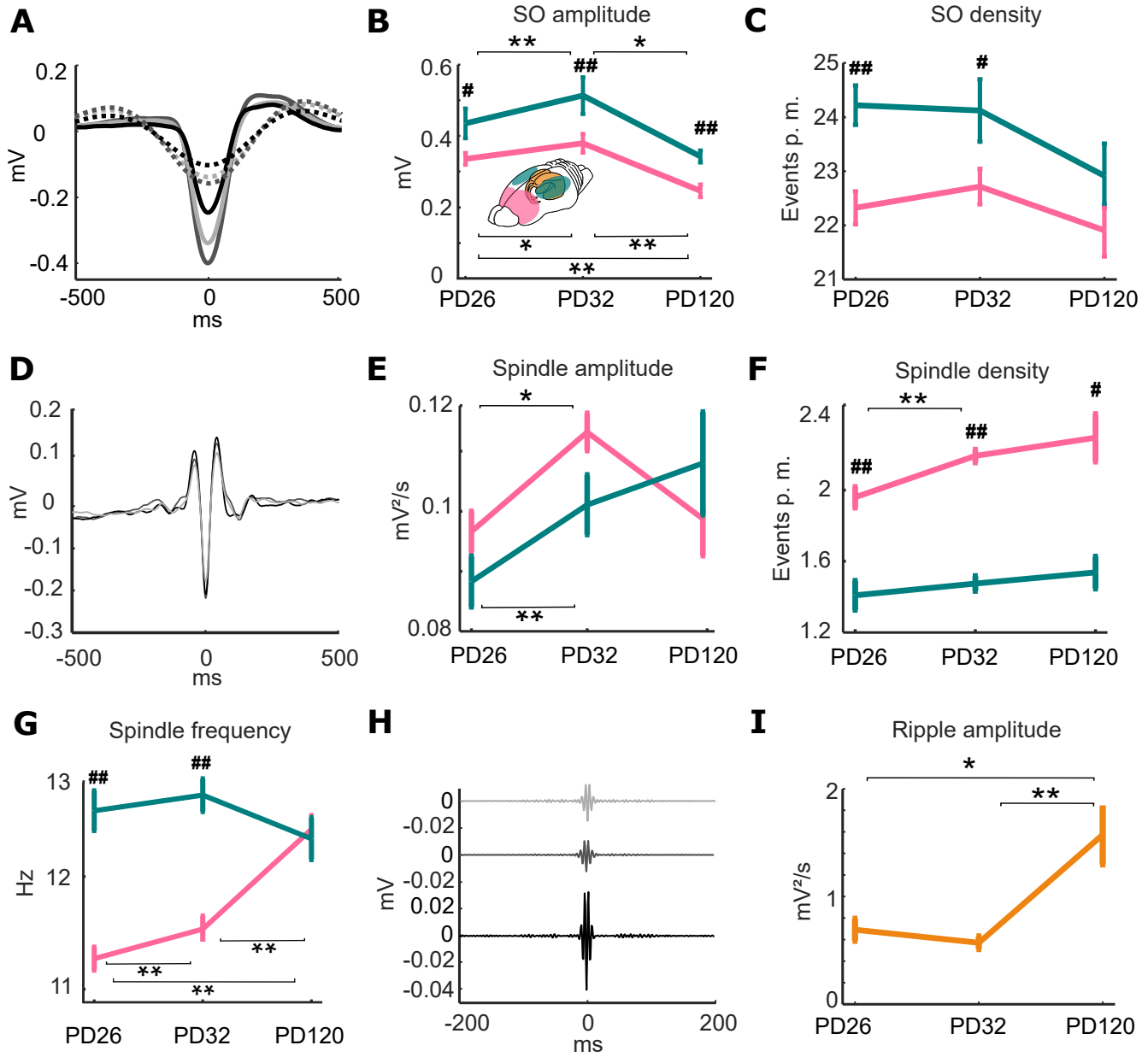
A
0.2
0
-0.2
-0.4
mV
-500
0
500
ms
B
SO amplitude
**
*
##
#
##
0.6
0.4
0.2
0
mV
*
**
**
PD26
PD32
PD120
C
SO density
##
#
25
24
23
22
21
Events p. m.
PD26
PD32
PD120
D
0.2
0.1
0
-0.1
-0.2
-0.3
mV
-500
0
500
ms
E
Spindle amplitude
*
0.12
0.1
0.08
mV²/s
**
PD26
PD32
PD120
F
Spindle density
**
#
##
##
2.4
2
1.6
1.2
Events p. m.
PD26
PD32
PD120
G
Spindle frequency
##
##
13
12
11
Hz
**
**
**
PD26
PD32
PD120
H
0
-0.02
0
-0.02
0.02
0
-0.02
-0.04
mV
-200
0
200
ms
I
Ripple amplitude
*
**
2
1
0
mV²/s
PD26
PD32
PD120

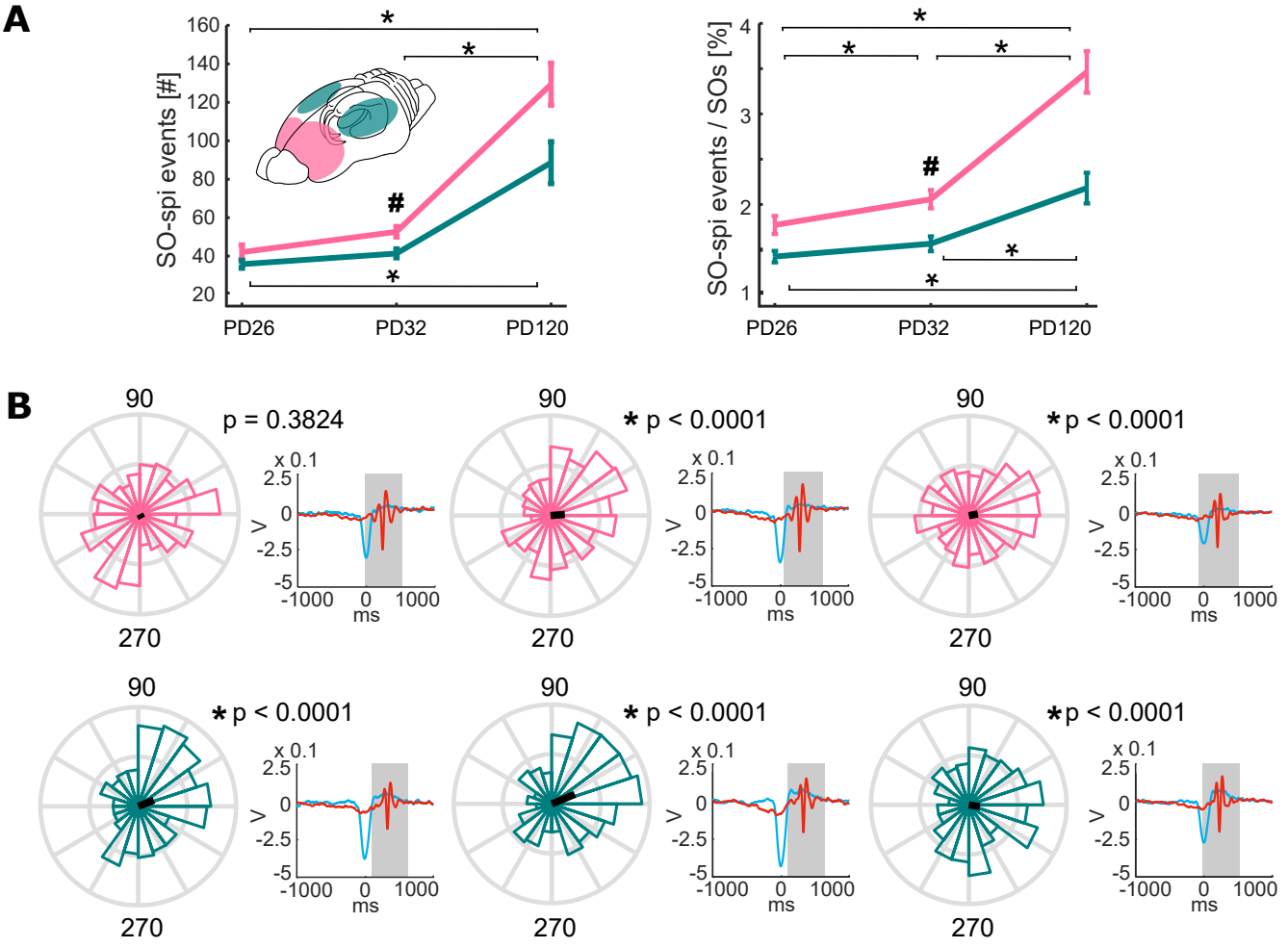
A
SO-spi events [#]
160
140
120
100
80
60
40
20
PD26
PD32
PD120
*
*
#
*
SO-spi events / SOs [%]
4
3
2
1
PD26
PD32
PD120
*
*
*
#
*
*
B
90
270
p = 0.3824
* p < 0.0001
* p < 0.0001
* p < 0.0001
* p < 0.0001
* p < 0.0001
x 0.1
2.5
0
-2.5
-5
V
-1000
0
1000
ms

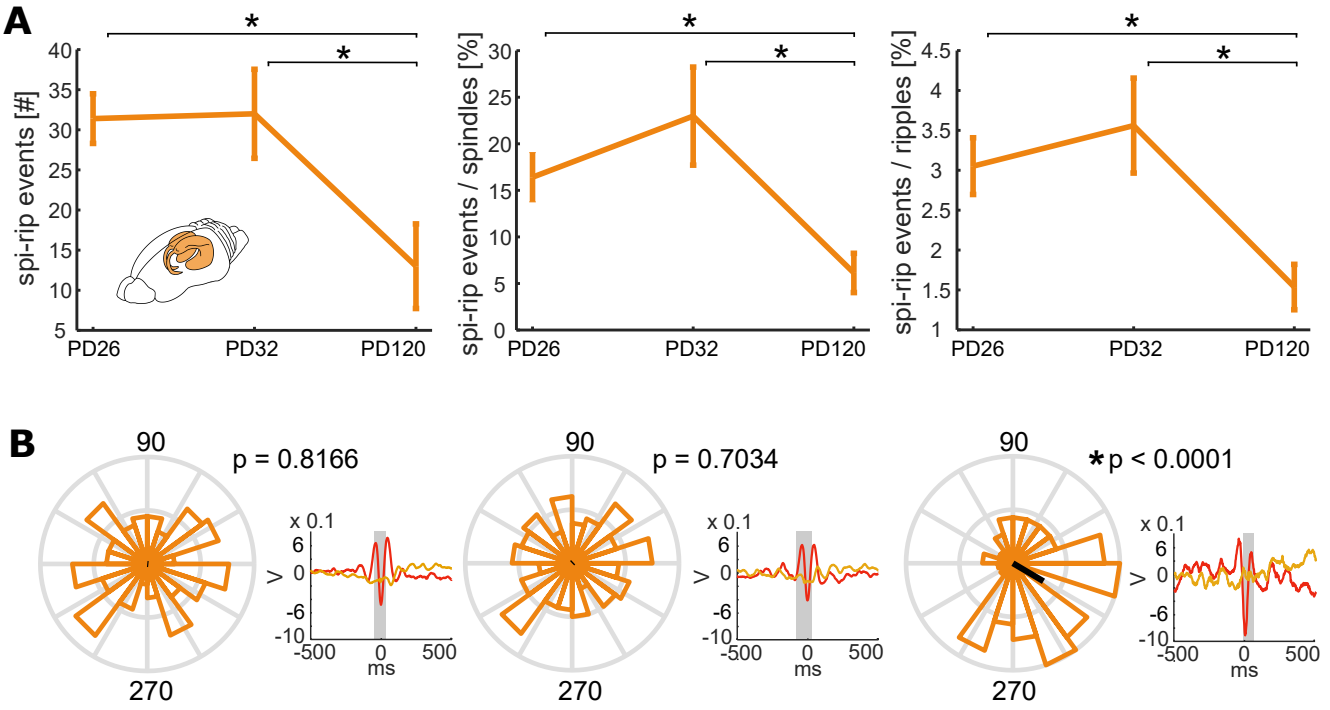
A
spi-rip events [#]
spi-rip events / spindles [%]
spi-rip events / ripples [%]
PD26
PD32
PD120
*
B
90
270
p = 0.8166
p = 0.7034
*p < 0.0001
x 0.1
mV
ms
-500
0
500

Supplementary materials:

Sleep Slow Oscillation-Spindle Coupling Precedes Spindle-Ripple Coupling During Development

Julia Fechner[1,*], María P. Contreras[1,*,#], Candela Zorzo[1,2], Xia Shan[1], Jan Born[1,3,4,5,†] and Marion Inostroza[1,†]

[1] Institute of Medical Psychology and Behavioral Neurobiology, University of Tübingen, Tübingen, Germany

[2] Laboratory of Neuroscience, Department of Psychology, Instituto de Neurociencias del Principado de Asturias (INEUROPA), University of Oviedo, Plaza Feijoo, Oviedo, Spain.

[3] German Center for Diabetes Research (DZD), Institute for Diabetes Research & Metabolic Diseases of the Helmholtz Center Munich at the University Tübingen (IDM), Germany

[4] Werner Reichert Center for Integrative Neuroscience, University of Tübingen, Tübingen, Germany

[5] German Center for Mental Health (DZPG), partner site Tübingen, Germany

* shared first authorship

[#] Present address: Leibniz Institute of Neurobiology, Magdeburg, Germany

† shared senior authorship

Correspondence to: Marion Inostroza or Jan Born

Emails: marion.inostroza@uni-tuebingen.de, jan.born@uni-tuebingen.de

Supplementary Table 1:

Stage	Time (min)		
	PD26	PD32	PD120
Wake	186.3 ± 19.5	191.0 ± 9.7	153.7 ± 13.4
SWS	139.9 ± 9.4	139.9 ± 7.0	171.5 ± 12.3
REM	41.6 ± 4.8	32.9 ± 3.1	29.4 ± 3.1
preREM	4.7 ± 0.6	6.4 ± 0.8	5.3 ± 1.0

Table S1: Mean (±standard deviation) time spent in wakefulness, SWS, REM sleep and preREM sleep (during a total of 360 minutes of recordings in each rat), for recordings at PD26, PD32 and PD120. All animals spent most time in SWS. The young animals (at PD26 and PD32) tended to spend less time in SWS than the adult rats (PD120; $p < 0.08$) possibly due to the fact that unlike in adult rats where a continuous 6-hour sleep record was assessed, in the young animals two 3-hour recordings were separated by a 5-min interval of enforced wakefulness.

Supplementary Table 2:

Test	Age	Recording site	Spindle Maximum	Spindle Onset
Rayleigh test	PD26	frontal	p = 0.3824	p = 0.1960
Rayleigh test	PD26	parietal	p < 0.0001	p < 0.0001
Rayleigh test	PD32	frontal	p < 0.0001	p < 0.0001
Rayleigh test	PD32	parietal	p < 0.0001	p < 0.0001
Rayleigh test	PD120	frontal	p < 0.0001	p < 0.0001
Rayleigh test	PD120	parietal	p < 0.0001	p < 0.0001
multi-sample test for equal median directions	PD26, PD32, PD120	frontal	p = 0.371	p < 0.002
multi-sample test for equal median directions	PD26, PD32, PD120	parietal	p = 0.062	p < 0.0003
multi-sample test for equal median directions	PD32, PD120	frontal	p = 0.1974	p < 0.002

Table S2: P-values of SO-spindle phase-locking analyses after SO-spindle events have been detected in frontal and parietal EEG recordings and in age groups PD26, PD32 and PD120, using spindle maximum or spindle onset.

Supplementary Figure 1:

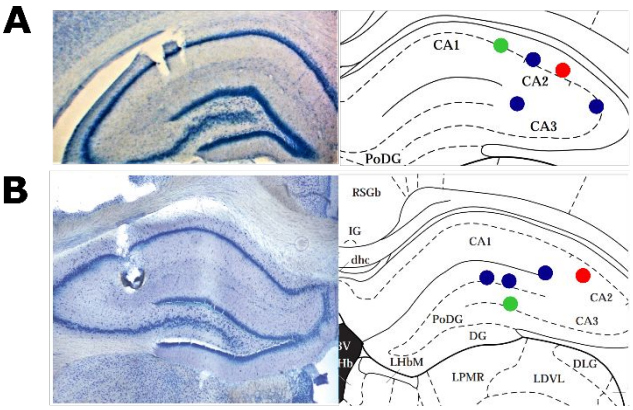

Figure S1: Coronal histological sections showing LFP electrode sites in the dHC. Dots show reconstructed electrode sites at **(A)** Bregma level -3.14 mm at age PD33 **(B)** and at Bregma level -3.12 mm after age PD120. Note, as there were differences in the location of electrodes in hippocampal subfields between the juvenile and adult groups of rats, in two supplementary control analyses we examined effects of age on ripples for the electrodes showing the smallest difference (marked in red) and the greatest difference in location (marked in green) between the age groups. Both analyses basically confirmed the age-dependent changes in ripples as observed for the whole groups, with a decrease in ripple amplitude from PD26 to PD32 and a distinct increase in amplitude at adulthood ($p < 0.001$ for respective ANOVA age main effects). Both analyses also confirmed the strong decrease in the number of ripple-spindle events from PD26 to adulthood as well as the lack of phase coupling of ripples to the spindle cycle at PD26 ($p > 0.722$, Rayleigh test) and PD32 ($p > 0.266$). The pattern of changes at these electrode sites closely matching with that observed for the entire groups suggests that the age-dependent changes in ripples reported here are largely independent of the precise hippocampal subfield location of the electrodes.

Supplementary Figure 2:

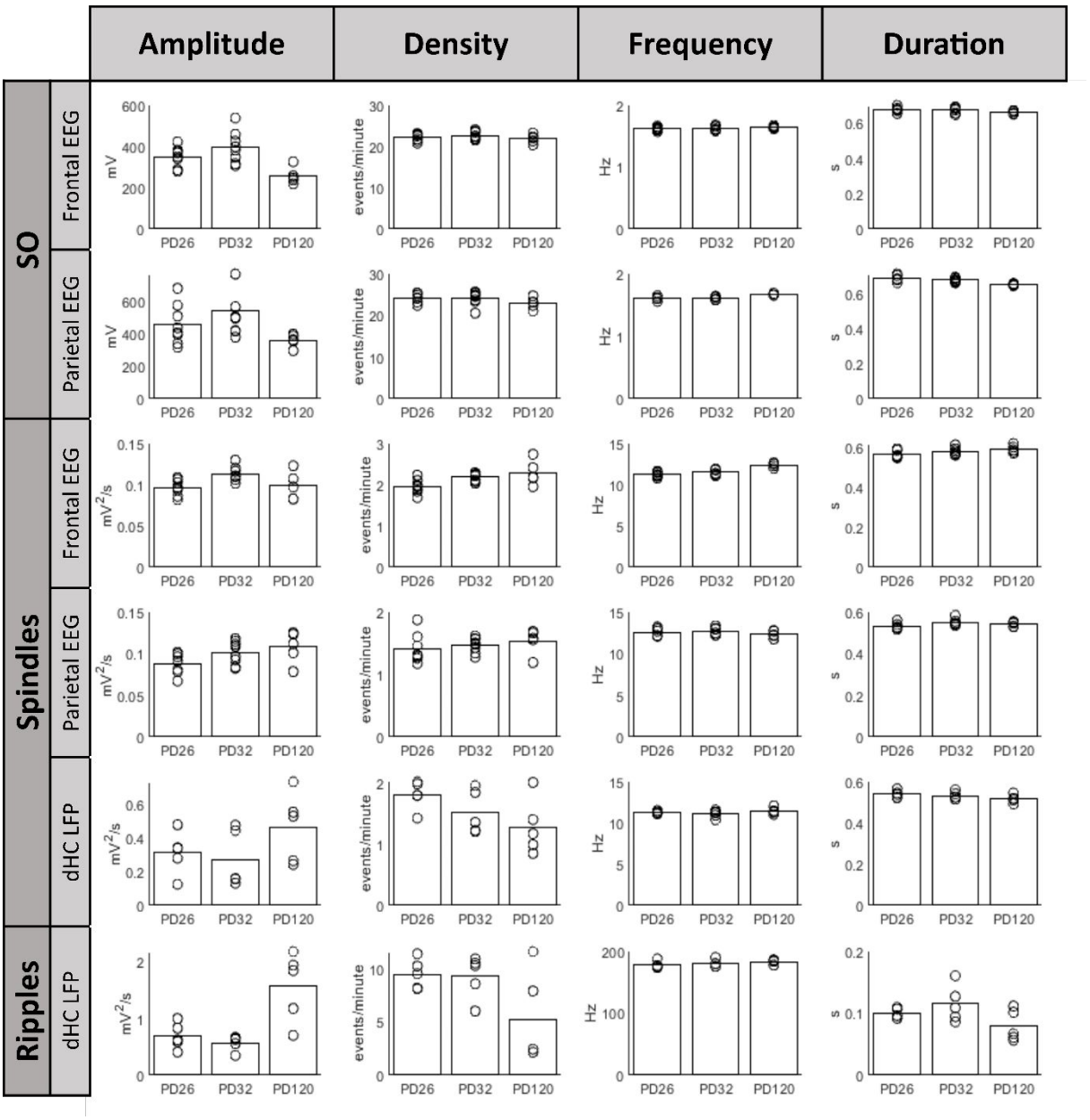

Figure S2: Distribution of the quantified parameters of each animal.

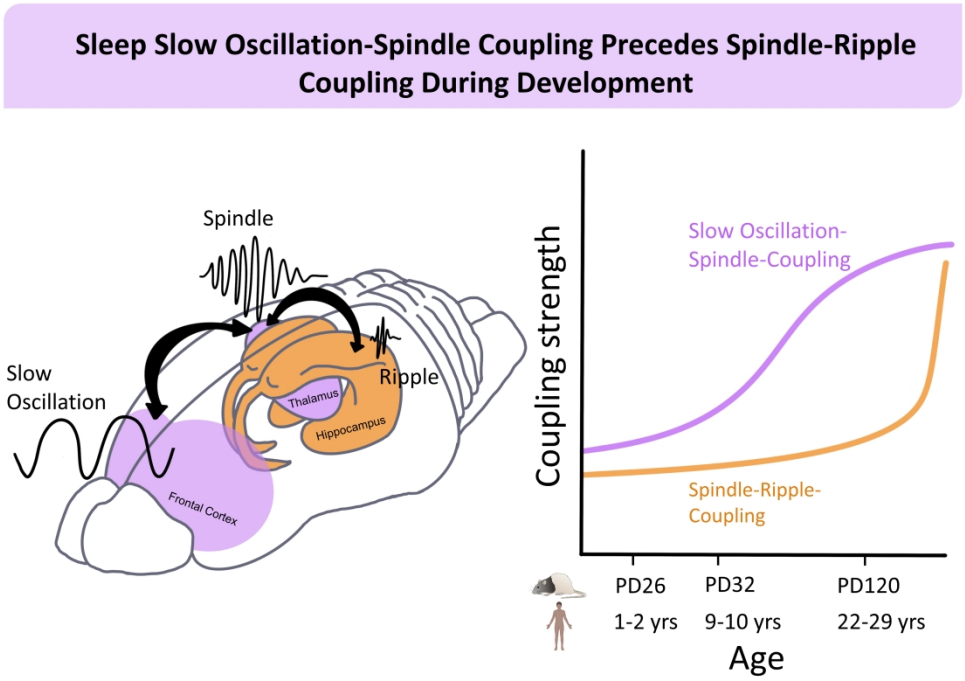

980x700mm (96 x 96 DPI)